OATAO
Open Archive Toulouse Archive Ouverte

Open Archive Toulouse Archive Ouverte (OATAO)

Stratigraphy, sedimentology

Cliff retreat and sea bed morphology under monochromatic wave forcing: Experimental study

Recul de falaise et morphologie du fond sableux sous un forçage de houle monochromatique : étude expérimentale

Bastien Caplain [a,*,b], Dominique Astruc [a,b], Vincent Regard [c,d,e], Frédéric Y. Moulin [a,b]

[a] INPT, UPS, IMFT, Université de Toulouse, allée Camille-Soula, 31400 Toulouse, France
[b] CNRS, IMFT, 31400 Toulouse, France
[c] UPS (OMP), GET, Université de Toulouse, 14, avenue Edouard-Belin, 31400 Toulouse, France
[d] CNRS, GET, 31400 Toulouse, France
[e] IRD, GET, 31400 Toulouse, France

Wave flume experiments have been performed to investigate a sandy cliff recession under monochromatic wave forcing. We varied the wave climate through the wave energy flux F and the surf similarity parameter ξ. The various processes of the cliff erosion cycle are depicted. The sea bed evolution mostly depends on the surf similarity parameter ξ. Steep planar ($\xi > 0.7$), gentle planar ($0.5 < \xi < 0.7$) and bared ($\xi < 0.5$) profiles are observed. We observed different bar dynamics, including steady and unsteady self-sustained oscillating states. Then we analyze the role of the eroded material on the cliff recession rate. We show that the cliff recession rate increases with the wave energy flux. Moreover, for a given wave energy flux, it is larger for a gentle planar profile than for a bared profile. However it is similar for both a bared profile and a steep planar profile. The cliff recession rate is not a monotonic function of the cliff height as the type of bottom profile influences the wave energy at the cliff.

Keywords:
Cliff erosion
Sea bed profile
Experimental modelling

R É S U M É

Des expériences en canal à houle ont été réalisées pour étudier la récession d'une falaise de sable sous un forçage de vagues monochromatiques. Nous avons fait varier le climat de houle à travers le flux d'énergie de houle F et le paramètre de similitude de « surf » ξ. Les différents processus du cycle d'érosion de falaise sont identifiés. L'évolution du fond dépend essentiellement du paramètre de similitude de surf ξ. Des profils plans à pente raide ($\xi > 0,7$), plans à pente douce ($0,5 < \xi < 0,7$) et à barre ($\xi < 0,5$) sont observés. Nous avons observé différentes dynamiques des barres, notamment des états stables et des états oscillants auto-entretenus. Puis nous analysons le rôle du matériau érodé sur la vitesse de récession de falaise. Nous montrons que la vitesse de récession de falaise augmente avec le flux d'énergie de houle. De plus, pour un flux d'énergie de houle donné, elle est plus forte pour un profil plan à pente douce que pour un profil à barre. Cependant, elle est semblable pour un profil à barre et pour un profil plan à pente raide. La vitesse de récession de falaise n'est pas une fonction monotone de la hauteur de falaise, puisque le type de profil du fond influence l'énergie de houle au niveau de la falaise.

Mots clés :
Érosion de falaise
Profil du fond
Modélisation expérimentale

---

1. Introduction

The coastlines of the Earth are composed of about 80% of rocky coasts (Emery and Kuhn, 1982). These coasts are composed of either consolidated or unconsolidated rocks such as clay (Collins and Sitar, 2008). It is crucial to be able to forecast cliff recession rate as a function of the local forcing parameters and the different underlying physical mechanisms should be understood. The main factor controlling cliff erosion is wave attack, but to mention a few others, tidal cycles (Kanyaya and Trenhaile, 2005), lithology, and living organisms (Nesteroff and Mélières, 1967) also play a role. In this work, we focus on erosion controlled by wave attack.

Wave-driven cliff erosion involves several processes. The wave impact creates a notch (Trenhaile et al., 1998) at the bottom of the cliff which grows until the weight of the overlying cliff exceeds the material strength, causing cliff collapse (e.g. Hampton, 2002; Young and Ashford, 2008). This collapse is responsible for cliff retreat and sediment supply to the beach. Then wave-driven collapsed material transport modifies the sea bed morphology. In turn, wave dynamics is changed by sea bed profile evolution (Walkden and Dickson, 2008).

Damgaard and Dong (2004) performed a wet sand cliff erosion experiment in a wave basin with a constant slope. The cliff was located on a flat platform. Incident waves were generated with a wave maker allowing variable wave incidence. They concluded that the cliff recession rate exponentially decreases in time for normal waves and seems to be constant for oblique waves. In addition, the recession rate increases with wave height and period and decreases with cliff height.

The aim of the present work is to analyze the cliff erosion dynamics within scales compatible with laboratory scale because such in situ analysis is made difficult by the large time scales involved in natural systems. Here, the time scale considered is of the order of a day and the spatial scale is metric. We performed experiments in a wave flume where the wet sand cliff was located upon a constant slope (Fig. 1). We will introduce experimental set up and parameters in the next section. Then the self-organization of the sea bed morphology is studied. Then, the influence of the wave properties and sediment supply on cliff recession rate is analyzed. The results are discussed before conclusions are drawn.

2. Experimental setup/method

In the present work, the experiments were carried out in a 5 m-long, 14 cm-wide and 25 cm-high wave flume where only normal incident waves are allowed (Fig. 1). The flume is equipped with a flap wave paddle producing monochromatic waves with a height up to 5 cm and periods between 0.5 s and 2 s. The offshore water depth is d = 15 cm. A hard nearshore slope of tan(β) = 1/10 is used. The wet sand cliff is built on the slope (Fig. 1) with a cliff length L_c = 40 cm. The cliff height h is measured from the free surface at rest to the cliff top. Calcite sand with a median grain diameter d_{50} = 0.41 mm and a density ρ_s = 2.76 g/cm³ (fall velocity in water of w_s = 5.45 cm/s) is used. After a cliff drainage of about 2 h, the flume is filled up to d = 15 cm. The bottom of the cliff is submerged and an initial notch appears during the filling of the tank. Then, the wave maker is activated.

Free surface position is measured by three capacitive probes (100 Hz sampling) located offshore (Fig. 1). Two PCO 2000 cameras have been used, one on the side of the flume (with a field of view 1 m × 25 cm) (Fig. 3c and 3d) to detect the water free surface and the bed and cliff positions, the other one above the flume (with a field of view 40 cm × 15 cm) to measure the cliff top position. At the beginning of each experiment (for 4 h), the video sampling rate is close to the wave frequency as the system dynamics is fast. Then the sampling rate is decreased to about 1/10 of this frequency until the end of the experiment. From video records, the free surface and the bed positions are measured.

The monochromatic wave climate is characterized by two parameters, the surf similarity parameter ξ and the incident wave energy flux F which are written:

$$\xi = \frac{\tan(\beta)}{\sqrt{H/L}} \tag{1}$$

$$F = E.c_G \tag{2}$$

with E the linear wave energy density E = 1/8 $\rho\, g\, H^2$, where ρ is the water density and g is the gravity acceleration, and c_G the corresponding group velocity. Tan(β) is the bottom slope, H the wave height, L the wave length.

Cliff erosion rate and bed evolution are studied as a function of incident wave energy, wave shape and cliff height. The conditions of experiments carried out are shown in Table 1.

3. Results

At the beginning of the experiments, cliff retreat is very fast and collapsed sediment quickly creates a sandy platform on the slope. In case 1 (reference experiment), the sea bed morphology rapidly evolves to a bared profile and plunging breaking waves are observed. Afterwards, the sand cliff recession rate decreases towards a steady profile (Fig. 2).
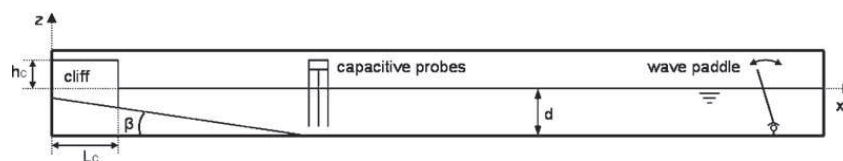

Fig. 1. Experimental device.

Fig. 1. Dispositif expérimental.

Table 1
Experimental conditions.

Tableau 1
Conditions expérimentales.

Cases	Surf similarity parameter ξ	Wave energy flux F (W/m)	Cliff height h_c (cm)	Dean parameter Ω	Mean reflection coefficient (%)
1-A	0.38	1.23	8	1.14	9
1-B	0.39	1.17	8	1.10	8
1-C	0.40	1.14	8	1.09	11
1-D	0.40	1.09	8	1.07	10
2	0.39	0.71	8	1.05	6
3	0.38	1.89	8	1.22	12
4	0.46	1.63	8	0.89	11
5	0.55	1.23	8	0.58	18
6	0.56	1.04	8	0.53	12
7	0.56	0.88	8	0.63	12
8	0.79	0.73	8	0.34	34
1–5	0.40	1.12	5	1.07	9
1–10	0.39	1.27	10	0.97	14
6–10	0.54	1.04	10	0.66	9

3.1. Bottom morphology

The influence of the wave parameters (F, ξ) (Fig. 3a) on the sea bed morphology is studied with a series of experiments carried out with the same cliff height $h_c = 8$ cm. Three different types of sea bed morphology are distinguished depending more on ξ rather than on F (Fig. 3):

- Planar and steep profiles for ξ greater than 0.7 (Fig. 3b). Waves break only when interacting with the backwash at the outward edge of the platform.
- Planar and gentle profiles for ξ between 0.5 and 0.7 (Fig. 3c). Waves break above the outward edge of the platform. Spilling breakers are observed.
- Bared profiles for ξ less than 0.5 (Fig. 3d). We observed either one (case 2) or two (outer and inner) sandbars (cases 1-A, 1-B, 1-C, 1-D, 3 and 4) depending on F. Breaking waves are of plunging type located above the outer sandbar.

Most of the observed profiles reach a steady state (see Fig. 2, for example). However, some cases evolve towards
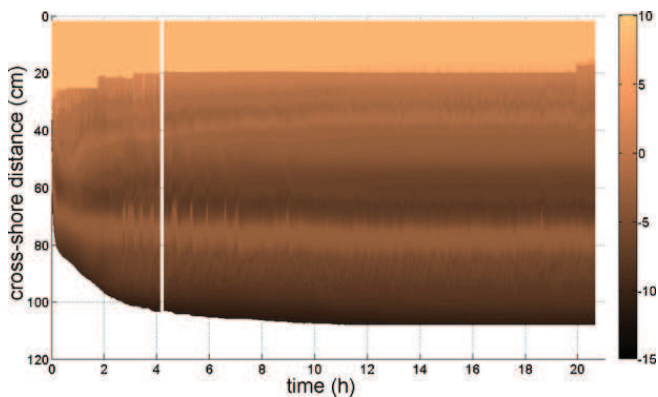

Fig. 2. Spatial and temporal evolution of sea bed morphology for case 1-A; color scale represents the bottom elevation (in cm).

Fig. 2. Évolution spatiale et temporelle de la morphologie du fond pour le cas 1-A ; l'échelle de couleur représente l'élévation du fond (en cm).

an unsteady state. For example, case 3 $(F, \xi) = (1.89, 0.38)$ characterized by a bared profile at high energy flux shows a self-sustained sandbar oscillation (Fig. 4a). After some time (7 h 30 min), sandbars begin to migrate, landward for the outer bar and seaward for the inner bar (Fig. 5). This migration lasts for about 80 min. The return motion is faster and lasts for only 20 min. Then, the system becomes stable again for about 1 h, before another oscillation starts. In sum, the oscillation period is about 2 h 30 min. Outer and inner sandbar excursions are about 16 and 5 cm, respectively. Another case of a self-sustained sandbar oscillation is observed for a higher cliff ($h_c = 10$ cm) with a lower wave energy flux ($[F, \xi] = [1.27, 0.39]$ close to the case 1-A). The system dynamics is somehow different as bar oscillations are in phase and symmetric and the oscillation frequency is higher than in the previous case (with a period of about 30 min) but the amplitudes are approximately the same (Fig. 4b).

3.2. Cliff recession rate

We study the cliff recession rate as a function of the wave parameters (F, ξ) and then as a function of the sediment supply. We see on Fig. 6 that for a set of four different realizations of the same case in the (F, ξ) plan (cases 1-A, 1-B, 1-C, 1-D) and despite the fact that the collapse events are different, the final cliff positions are very close. The variability in final cliff position is close to the variability of F for the various experiments (about 10%). We thus conclude that the cliff recession dynamics is reproducible in our experiment. The cliff recession rate increases for increasing wave energy flux (Fig. 6a) as observed by Damgaard and Dong (2004). For a given energy flux, we changed the surf similarity parameter, and thus the sea bed morphology. Cliff recession is larger for a gentle planar profile (case 5: $0.5 < \xi < 0.7$) than for a bared profile (case 1-A: $\xi < 0.5$) (Fig. 6b). The final cliff position is the same for both a bared profile (case 2: $\xi < 0.5$) and a steep planar profile (case 8: $\xi > 0.7$) (Fig. 6b).

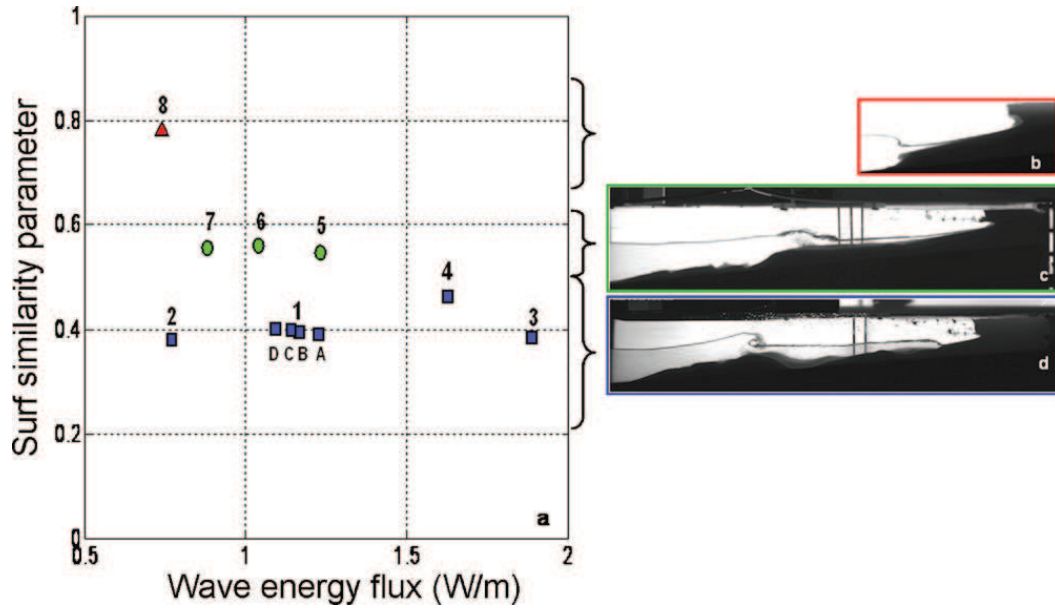The influence of sediment supply in the system is studied from two perspectives:

Fig. 3. (a) Studied waves regimes in the (F, ξ) plane; symbols represent the sea bed profile type: steep planar (triangles) or gentle (circles) planar profiles and bared profiles (squares). Examples of side views for each type of profiles are (b), (c) and (d), respectively.

Fig. 3. (a) Régimes de houle étudiés dans le plan (F, ξ) ; les symboles représentent le type de profil du fond : les profils plans à pente raide (triangles) ou à pente douce (cercles) et les profils à barre (carrés). Exemples de vues de côté pour chaque type de profil en (b), (c) et (d), respectivement.
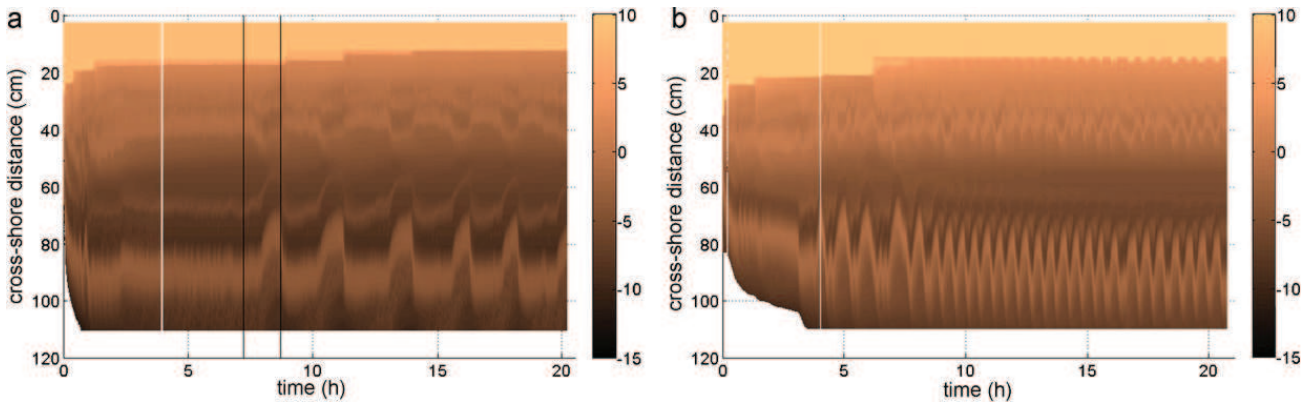

Fig. 4. Same as Fig. 2 for: (a) $(F, \xi) = (1.89, 0.38)$, $h_c = 8$ cm (case 3) and (b) $(F, \xi) = (1.27, 0.39)$, $h_c = 10$ cm (bared profiles); color scale represents the bottom and cliff elevation (in cm). Black lines indicate the profiles plotted in Fig. 5.

Fig. 4. Idem Fig. 2 pour : (a) $(F, \xi) = (1.89, 0.38)$, $h_c = 8$ cm (cas 3) et (b) $(F, \xi) = (1.27, 0.39)$, $h_c = 10$ cm (profils à barre) ; l'échelle de couleur représente l'élévation du fond et de la falaise (en cm). Les lignes noires indiquent les profils reportés sur la Fig. 5.

(i) the periodic removal of the sandbar;
(ii) the variation of the cliff height.

During a test where a bared profile develops (case 1: $F = 1.19$, $\xi = 0.39$), we removed the outer bar a couple of
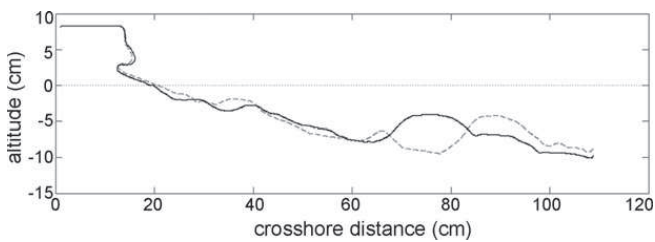

Fig. 5. Sea bed morphology for case 3 at about 7 h (grey dotted line) and at about 9 h (black full line) (Fig. 4a).

Fig. 5. Morphologie du fond pour le cas 3 à environ 7 h (ligne pointillée grise) et à environ 9 h (ligne pleine noire) (Fig. 4a).

minutes after each cliff collapse (Fig. 7). Comparing to the experiment with the same wave parameters but without sandbar removal (Fig. 8), it appears that the cliff retreat is more important when the sandbar is removed, featuring an almost constant recession rate.

The sediment supply in the system is also controlled by cliff height. For approximately the same wave climate (case 1), we performed experiments for three different cliff heights ($h_c = 5$, 8 and 10 cm). Fig. 9 shows that the total number of collapse events decreases with cliff height whereas average depth of a collapse event increases, and therefore average volume of a collapse event increases. Similarly to Damgaard and Dong (2004), we observed that for steady bared profiles the cliff recession rate decreases with increasing cliff height (5 cm-high and 8 cm-high cliffs, Fig. 10). In addition, the same conclusion is reached for gentle planar profiles (case 6; $h_c = 8$ and 10 cm).
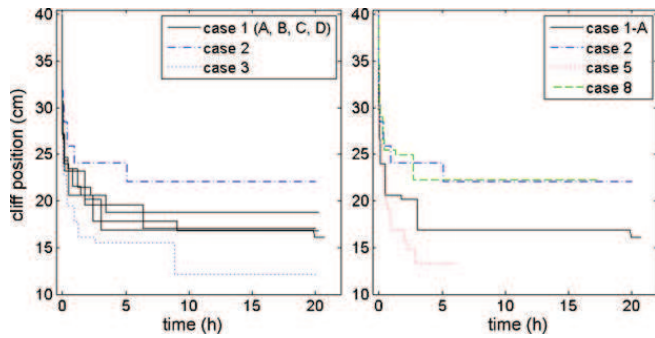
Fig. 6. Time evolution of cliff position for (a) different wave energy fluxes and (b) different surf similarity parameters. Initial cliff position is $L_c = 40$ cm.

Fig. 6. Évolution temporelle de la position de la falaise pour (a) différents flux d'énergie de houle et (b) différents paramètres de similitude de surf. La position initiale de la falaise est $L_c = 40$ cm.
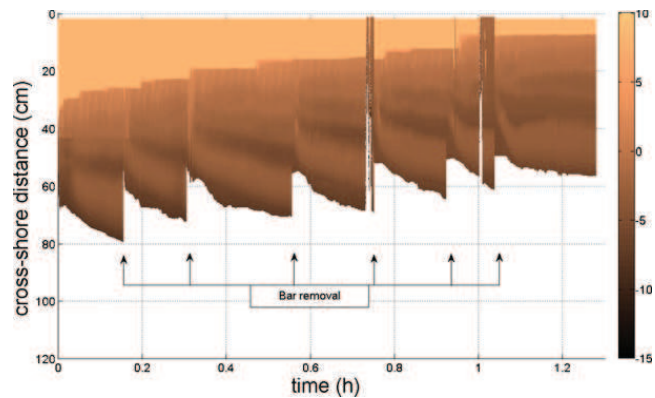

Fig. 7. Same as Fig. 2, for the case 1 with sandbar removal.

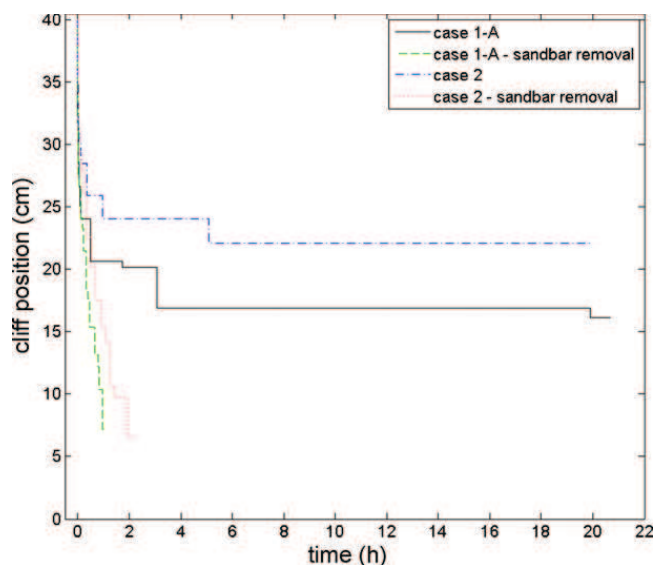**Fig. 7.** Idem Fig. 2, pour le cas 1, avec prélèvement de la barre de sable.

Fig. 8. Evolution of cliff position with and without sand bar removal. Cliff position is initially at $L_c = 40$ cm.

Fig. 8. Évolution de la position de falaise avec et sans prélèvement de la barre de sable. La position de la falaise est initialement à $L_c = 40$ cm.
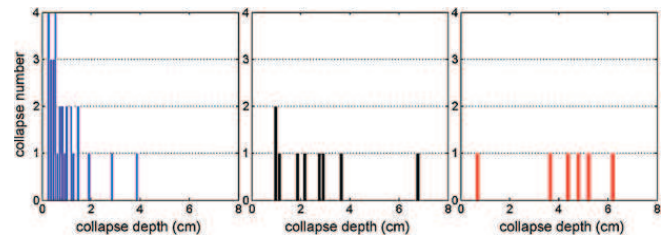

Fig. 9. Histogram of collapse depth for different cliff height (a): $(F, \xi) = (1.12, 0.40)$, $h_c = 5$ cm; (b): $(F, \xi) = (1.09, 0.40)$, $h_c = 8$ cm (case 1-B); (c): $(F, \xi) = (1.27, 0.39)$, $h_c = 10$ cm. Total number of collapse events: (a) 30; (b) 9; (c) 6. Average collapse depth: (a) 0.9 cm; (b) 2.6 cm; (c) 4.1 cm.

Fig. 9. Histogramme de la profondeur d'effondrement pour différentes hauteur de falaise (a) : $(F, \xi) = (1.12, 0.40)$, $h_c = 5$ cm ; (b) $(F, \xi) = (1.09, 0.40)$, $h_c = 8$ cm (cas 1-B) ; (c) : $(F, \xi) = (1.27, 0.39)$, $h_c = 10$ cm. Nombre total d'effondrements : (a) 30 ; (b) 9 ; (c) 6. Profondeur moyenne d'effondrement : (a) 0.9 cm ; (b) 2.6 cm ; (c) 4.1 cm.
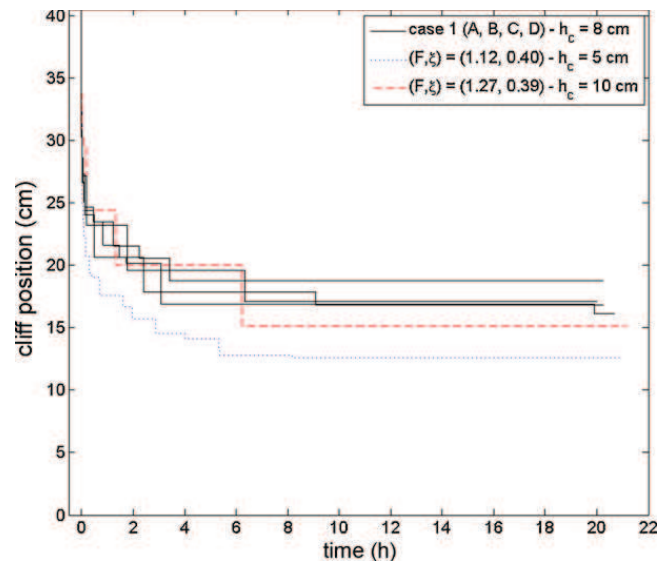

Fig. 10. Evolution of cliff position for three different cliff heights. Cliff position is initially at $L_c = 40$ cm.

Fig. 10. Évolution de la position de falaise pour trois différentes hauteurs de falaise. La position de la falaise est initialement à $L_c = 40$ cm.

We observe, however, that for bared profiles the cliff recession rate is larger for $h_c = 10$ cm than for $h_c = 8$ cm (Fig. 10) so that cliff retreat rate is not a monotonic function of cliff height. We should observe however that, the experiment with $h_c = 10$ cm is characterized by a self-sustained sandbar oscillation, unlike other two experiments.

We conclude that, as far as the bed morphology is steady, the cliff recession rate diminishes for increasing cliff height.

4. Discussion

We classified the different types of bed morphology as a function of wave climate. We observed three types of bottom profiles, planar profiles with either steep or gentle slope and bared profiles which mostly depend on surf similarity parameter value, i.e. on the type of wave breaking. The wave energy flux does not seem to influence

much the type of bed morphology (Fig. 3) but only the characteristic length and position of the morphological features.

Beach profiles classification has been proposed in the literature based on the Dean number value (Wright and Short, 1984). Here, we define the Dean number Ω with offshore wave parameters, as:

$$\Omega = \frac{H}{T.w_S} \tag{3}$$

As we use a single grain diameter in our experiments, Ω evolves similarly as ξ. It means that the bottom morphology depends mainly on the Dean number as observed by Wright and Short (1984). Steep planar profiles are thus observed for $\Omega < 0.4$, gentle planar profiles for $0.4 < \Omega < 0.8$ and bared profiles for $\Omega > 0.8$ (Table 1). This dependency of bottom morphology on Dean number is qualitatively similar to those of Wright and Short (1984), although the boundary values are not similar which may be explained by the different definition of the Dean number, ours expected to have smaller values than the one of Wright and Short (1984).

Most of the bottom profiles reached a steady state. Steady profiles have been previously obtained in laboratory experiments (Grasso et al., 2009; Kamalinezhad, 2004; Wang and Kraus, 2005). Sandbar migrates onshore for moderate waves conditions and offshore for very energetic waves conditions (Gallagher et al., 1998; Ruessink et al., 2003). Such migrations have been observed in laboratory experiments (Grasso et al., 2009; Hoyng, 2008), and in nature (Certain and Barusseau, 2005). Moreover, unsteady states have been observed for bared profiles at high wave energy fluxes. To our knowledge, sandbar oscillations have never been reported for a constant wave forcing.

The cliff recession rate has been studied as a function of wave forcing. We observed that it increases for increasing wave energy flux. However, there is no clear tendency of the influence of the surf similarity parameter on the cliff recession rate due to different types of sea bed morphology. The sea bed morphology appears as of primary importance on cliff recession control. Interestingly, using numerical models Dickson et al. (2007) reach the same kind of conclusion that is cliff recession is moderately affected by wave change and strongly affected by the beach/platform morphology.

A periodic removal of the sandbar leads to a constant cliff recession rate. This result is similar to Damgaard and Dong (2004)'s observations for oblique waves leading to a constant recession rate, in a system where the sediment is removed by transportation by the longshore current. For different cliff heights, we observed the volume of collapse events increases for increasing cliff height, and cliff recession rate is more important for small cliffs provided that the bottom morphology is steady. For the two stable sandbar cases (case 1: $h_c = 5$ and 8 cm), the final eroded volumes are very close whereas the final eroded volume is more important for the unstable profile ($h_c = 10$ cm). These findings may indicate that the bed profile destabilization could be related to the crossing of a threshold value for the eroded volume of cliff material. In addition it might show that the eroded volume for stable cases is almost independent on cliff height.

If we consider the cliff erosional process as an analogue to a beach nourishment plan, the results from our experiments may show that an increase of the sand nourishment volume will result in a decrease of beach erosion up to a certain amount of filled sand as the bed profile may become unstable and thus lead to a larger erosion at the end.

5. Conclusions

Wet sand cliff erosion by regular waves has been investigated in an experimental wave flume. Our results show that the type of self-organized sand bed morphology depends mainly on the surf similarity parameter. Steep planar profiles are observed for $\xi > 0.7$, gentle planar profiles for $0.5 < \xi < 0.7$ and bared profiles for $\xi < 0.5$. For bared profiles, we either observed steady or unsteady states in which the sandbars positions oscillate in the cross-shore direction.

The cliff recession rate depends mostly on the self-organized sea bed morphology. The cliff recession rate increases with the wave energy flux and is larger for a gentle planar profile than for a bared profile with the same wave energy flux. However, it appears to be similar for both bared and steep planar profiles with a constant wave energy flux. Thus, the sea bed morphology considerably influences the hydrodynamics and therefore the cliff recession. We have shown that the sediment supply plays an important role on cliff recession giving some insights into nourishment strategies.

References

Certain, R., Barusseau, J.P., 2005. Conceptual modeling of sand bars morphodynamics for a microtidal beach (Sète, France). Bull Soc. geol. France 176 (4), 343–354.

Collins, B.D., Sitar, N., 2008. Processes of coastal bluff erosion in weakly lithified sands, Pacifica, California, USA. Geomorphology 97, 483–501.

Damgaard, J.S., Dong, P., 2004. Soft cliff recession under oblique waves: physical model tests. Journal of waterway, port, coastal and ocean engineering 130 (5), 234–242.

Dickson, M.E., Walkden, M.J.A., Hall, J.W., 2007. Systemic impacts of climate change on an eroding coastal region over the twenty-first century. Climatic Change 84 (2), 141–166.

Emery, K., Kuhn, G., 1982. Sea cliffs: their processes, profiles, and classification. Geol. Soc. Am. Bull. 93 (7), 644–654.

Gallagher, E.L., Elgar, S., Guza, R.T., 1998. Observations of sand bar evolution on a natural beach. J. Geophys. Res. 103 (C2), 3203–3215.

Grasso, F., Michallet, H., Barthélemy, E. and Certain, R. 2009. Physical modeling of intermediate cross-shore beach morphology: transients and equilibrium states. J. Geophys. Res., 114, C09001.

Hampton, M.A., 2002. Gravitational failure of sea cliffs in weakly lithified sediment. Environmental and Engineering Geoscience 8 (3), 175–191.

Hoyng, C., 2008. Erosive and accretive coastal response. MSc. Thesis, WL Delft Hydraul, Deltft, Netherlands.

Kamalinezhad, M. 2004. Plages en équilibre morphologique et hydrodynamique associés. PhD Thesis, Institut national polytechnique de Grenoble, France.

Kanyaya, J.I., Trenhaile, A.S., 2005. Tidal wetting and drying on shore platforms: an experimental assessment. Geomorphology 70, 129.

Nesteroff, W.D., Mélières, F., 1967. L'érosion littorale du pays de Caux. Bull Soc. geol. France 7, 159–169.

Ruessink, B.G., Walstraa, D.J.R., Southgate, H.N., 2003. Calibration and verification of a parametric wave model on barred beaches. Coastal Engineering 48, 139–149.

Trenhaile, A.S., Pepper, D.A., Trenhaile, R.W., Dalimonte, M., 1998. Stacks and notches at Hopewell Rocks, New Brunswick, Canada. Earth Surface Processes and Landforms 23, 975–988.

Walkden, M., Dickson, M., 2008. Equilibrium erosion of soft rock shores with a shallow or absent beach under increased sea level rise. Marine Geology 275, 75–84.

Wang, T., Kraus, N.C., 2005. Beach profile equilibrium and patterns of wave decay and energy dissipation across the surf zone elucidated in a large-scale laboratory experiment. J. Coastal Res. 21 (3), 522–534.

Wright, L.D., Short, A.D., 1984. Morphodynamic variability of surf zones and beaches: a synthesis. Marine Geology 56, 93–118.

Young, A.P., Ashford, S.A., 2008. Instability investigation of cantilevered seacliffs. Earth Surface Processes and Landforms 33, 1661–1677.